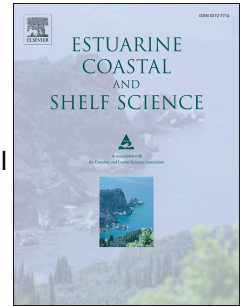


Journal Pre-proof

Morphological evolution of a non-engineered managed realignment site following tidal inundation

Jonathan Dale, Heidi M. Burgess, Maureen J. Berg, Conor J. Strong, Niall G. Burnside



PII: S0272-7714(21)00362-0

DOI: <https://doi.org/10.1016/j.ecss.2021.107510>

Reference: YECSS 107510

To appear in: *Estuarine, Coastal and Shelf Science*

Received Date: 10 February 2021

Revised Date: 14 July 2021

Accepted Date: 15 July 2021

Please cite this article as: Dale, J., Burgess, H.M., Berg, M.J., Strong, C.J., Burnside, N.G., Morphological evolution of a non-engineered managed realignment site following tidal inundation, *Estuarine, Coastal and Shelf Science* (2021), doi: <https://doi.org/10.1016/j.ecss.2021.107510>.

This is a PDF file of an article that has undergone enhancements after acceptance, such as the addition of a cover page and metadata, and formatting for readability, but it is not yet the definitive version of record. This version will undergo additional copyediting, typesetting and review before it is published in its final form, but we are providing this version to give early visibility of the article. Please note that, during the production process, errors may be discovered which could affect the content, and all legal disclaimers that apply to the journal pertain.

© 2021 Published by Elsevier Ltd.

Jonathan Dale: Conceptualisation, Methodology, Investigation, Formal Analysis, Writing – Original Draft, Visualisation. Heidi M Burgess: Investigation, Resources, Project Administration, Funding acquisition. Maureen J Berg: Investigation, Writing – Review & Editing. Conor J Strong: Software, Data Curation. Niall G Burnside: Software, Formal analysis, Investigation, Resources, Writing – Review & Editorial.

Journal Pre-proof

1 **Morphological evolution of a non-engineered managed realignment**
2 **site following tidal inundation**

3
4 Jonathan Dale^{1*}, Heidi M Burgess², Maureen J Berg², Conor J Strong², Niall G Burnside²

5

6 ¹ Centre for Agroecology, Water and Resilience (CAWR), Coventry University, Coventry, CV8 3LG, UK.

7 ²Centre for Aquatic Environments, University of Brighton, Brighton, BN2 4GJ, UK.

8

9 *Corresponding Author:

10 Jonathan Dale

11 School of Energy, Construction and Environment, Coventry University, John Laing Building, Much

12 Park Street, Coventry, UK, CV1 2LT

13

14 Email: jonathan.dale@coventry.ac.uk

15 Submitted to *Estuarine, Coastal and Shelf Science*

16

17 Keywords

18 Sedimentation rates; coastal geomorphology; coastal wetlands: small-Unmanned Aerial System

19 **Abstract**

20 There is growing evidence that managed realignment (MR) sites have lower biodiversity than natural
21 saltmarshes, which has been associated with differences in the physical function and morphological
22 evolution following site breaching. This evidence has been derived from MR sites previously used for
23 intensive arable agriculture or modified during site construction. Therefore, the development of
24 these sites may not be representative of the sedimentological evolution that would have otherwise
25 occurred. This paper presents analysis of high spatial resolution digital surface models derived from
26 the images collected using a small-unmanned aerial system from a non-engineered MR site at Cwm
27 Ivy Marsh, Gower Peninsula, Wales. These models are examined alongside a novel combination of
28 high frequency measurements of the rate and patterns of sedimentation, suspended sediment
29 concentration (SSC), and the sub-surface structure and geochemical profiles. Results indicated that
30 although the site became topographically less variable over a four year period, the intertidal
31 morphology developed through an increase in the abundance of higher order creek systems and
32 sediment being deposited at a rate of between 3 to 7 cm / year. The SSC followed an inverse pattern
33 to water depth, with bed elevation increasing and then decreasing during both the flood and ebb
34 tidal phases. Analysis of the sediment subsurface geochemical composition indicated redox profiles
35 similar to natural intertidal environments; evidence of a fluctuating water table was found at a
36 saltmarsh site, in comparison to waterlogging identified at an anoxic mudflat site. These findings
37 provide a new insight to the sedimentological processes in a MR site without the influence of
38 landscaping or site engineering prior to site-breaching, which can be used to inform the design of
39 future MR sites.

40 **1 Introduction**

41

42 Coastal wetlands, such as saltmarshes and mudflats, provide a number of important ecosystem
43 services including habitats for juvenile fish species, water quality regulation and wave attenuation
44 (Barbier et al., 2011). However, there has been a global decline in the extent of these habitats
45 (Adam, 2002; Barbier et al., 2011) as a result of loss and degradation caused by pollution,
46 urbanisation, land claim, changes in sediment supply, and erosion driven by sea level rise.
47 Subsequently, there are a number of schemes that have been implemented to restore and
48 compensate for the loss of intertidal saltmarsh habitat (Callaway, 2005). One approach, which has
49 become the preferred option in Europe and North America, is managed realignment (MR); where
50 sea defences are deliberately breached allowing tidal inundation of the previously defended
51 terrestrial land. MR is usually performed on low lying land that has previously been reclaimed for
52 agricultural purposes (French, 2006), and is often of lower economic value than the cost of
53 maintaining the external flood defence and protection schemes.

54

55 Following tidal inundation, saltmarsh plants and invertebrate species have been found to colonise
56 relatively quickly (Garbutt et al., 2006; Mazik et al., 2010; Wolters et al., 2005). However, at multiple
57 sites, the diversity of key plant species has been recognised to not be equivalent to natural saltmarsh
58 communities (Mossman et al., 2012). This has been associated with differences in sub-surface
59 sediment structure due to agricultural activities, such as ploughing, leading to poor drainage and
60 anoxic conditions (Spencer et al., 2017; Tempest et al., 2015). As a result, these sites may not be
61 delivering the targeted level of ecosystem services such as carbon storage (Moreno-Mateos et al.,
62 2012) or wave attenuation (Moller et al., 2014; Moller and Spencer, 2002; Rupprecht et al., 2017).
63 Site design often includes a mosaic of morphological features including channels, raised areas and
64 lowered sections to encourage a range of intertidal habitat, utilising the distinct elevational niches of

65 different saltmarsh species (e.g. Masselink et al., 2017; Sullivan et al., 2017). Consequently, elevation
66 is considered to be the key physical parameter in the design of MR sites (Howe et al., 2010).
67 However, this approach does not consider post-site breaching changes and the rate of
68 sedimentation. For example, at Paull Holme Strays (Humber estuary, UK) rapid accretion of sediment
69 occurred due to the high suspended sediment load in the Humber estuary (Mazik et al., 2010;
70 Wolanski and Elliott, 2016). Furthermore, at the Medmerry Managed Realignment Site (West Sussex,
71 UK) artificially lowered areas accreted at a faster rate than anticipated due to the internal re-
72 distribution of sediment following site breaching (Dale et al., 2017). In both of these cases, accretion
73 of sediment resulted in the loss of lower elevation environments targeted by the scheme, and did
74 not result in the creation of the range of intertidal habitat to the extent intended.

75

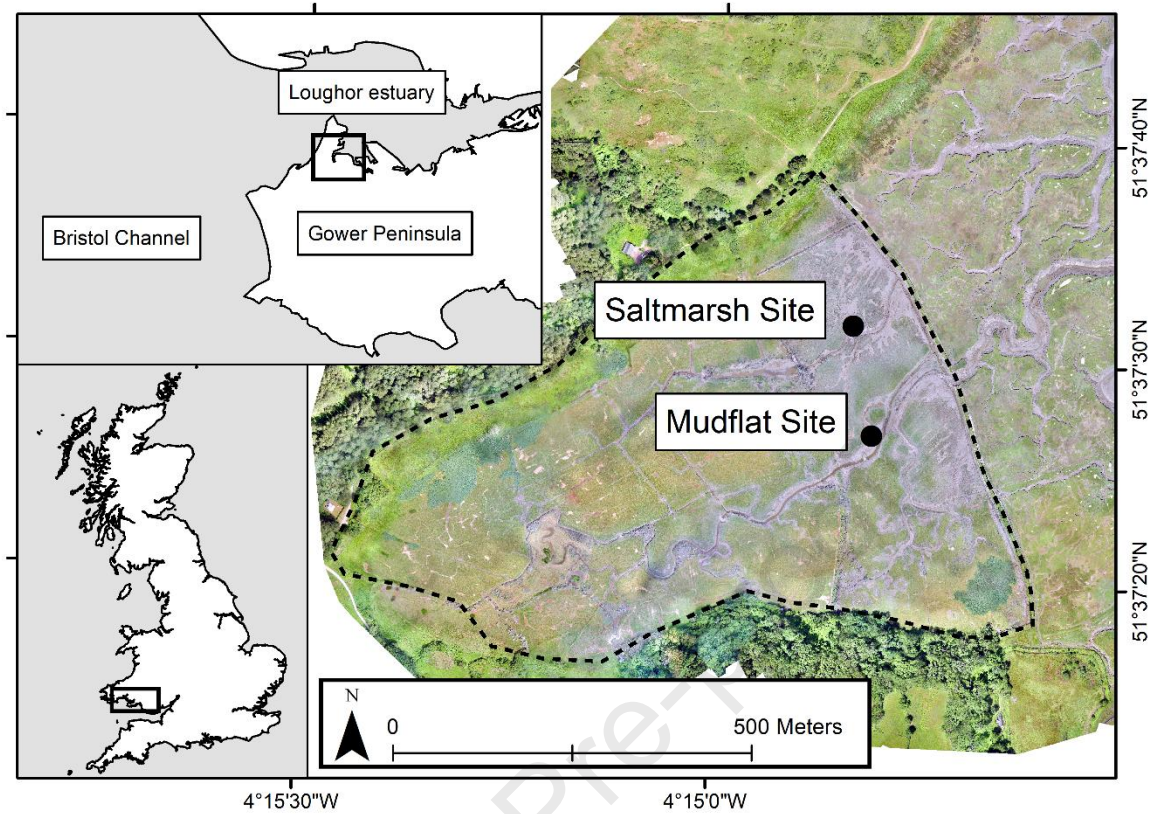
76 Predictions of a site's morphological evolution following inundation tend to be derived from
77 theoretical models based on observations of established saltmarshes (e.g. Allen, 2000), or post-site
78 breaching measurements of the rate of accretion (e.g. Dale et al., 2017; Spencer et al., 2017; Spencer
79 et al., 2008). However, empirical measurements from MR sites tend to be focused on sites that have
80 undergone a considerable amount of landscaping and engineering works during site construction
81 prior to site breaching, such as the creation of artificial drainage channels and changes in elevation
82 to encourage a range of habitat types (e.g. Burgess et al., 2014; Dale et al., 2017). As a result of the
83 changes to the elevation, morphology and drainage systems caused by the pre-breach landscaping,
84 these sites may not provide a realistic representation of the natural patterns and rates of
85 sedimentation following intertidal inundation. Furthermore, these studies have relied on traditional
86 surveying techniques, such as differential GPS and LiDAR (e.g. Chirol et al., 2018; Lawrence et al.,
87 2018). As a result, small (but important) changes in morphology such as embryonic creek formation
88 and the availability of distinct elevation niches, which are important for topography variability and
89 therefore plant diversity (e.g. Morzaria-Luna et al., 2004), are likely to have been missed. To address

90 these shortcomings, Dale et al. (2020) demonstrated the benefits of using repeat high resolution
91 digital surface models (DSMs) to examine morphological change in MR sites and intertidal wetlands
92 more widely. These authors produced DSMs using the emerging low-cost photogrammetric method
93 Structure-from-Motion, on images collected using a small-unmanned aerial system (sUAS), in order
94 to identify the morphological evolution. Nonetheless, their study focused on a specific area under
95 2000 m² and known to be developing morphologically, and failed to provide a holistic evaluation of
96 morphological changes across the entire site as it developed.

97

98 Therefore, there is a need for inclusive high resolution, *full-site* studies of recently breached non-
99 engineered MR sites to assess the morphological evolution without the influence of extensive (and
100 costly) site design and engineering works. To address this requirement, this study presents a whole
101 site analysis of a recently breached non-engineered MR site at Cwm Ivy Marsh, Gower Peninsula,
102 Wales. Specifically, the rate and spatial variability of the morphological evolution through
103 measurements of the morphological change, drainage network development and sediment
104 accretion and erosion across the site are evaluated via topographic surveys collecting using a sUAS.
105 These measurements are combined with analysis of the suspended sediment concentration (SSC) in
106 relation to the pattern of sedimentation (Dale et al., 2017), to evaluate the variability in the
107 deposition and supply of sediment over a tidal cycle. In addition, the preservation of the terrestrial
108 surface, and its influence on the physio-chemical evolution of the sediment sub-surface, is assessed
109 through sediment core analysis.

110



111

112 Figure 1: Orthophotography of Cwm Ivy Marsh derived from the July 2019 small-Unmanned Aerial
 113 System survey, the location of the saltmarsh and mudflat sites, and the regional and national setting
 114 (both insert). The site outline is marked by the dashed black line, with the external saltmarsh visible
 115 to the northeast and the sand dunes to the north and northwest.

116

117 2 Methods

118

119 2.1 Study Site

120

121 Cwm Ivy Marsh is situated on the Gower Peninsula (Figure 1), on the northern coast of the Bristol
 122 Channel; a major inlet on the south west coast of the UK which separate south Wales from southern

123 England. The site, which is located in the Loughor estuary, is banked by sand dunes and the open
124 coast to the north and northwest, and an expansive area of saltmarsh to the northeast. Tidal waters
125 are fed to the site through external marsh's dendritic creek network; there is limited freshwater
126 input from springs from the cliffs behind the site. The site, which had previously been reclaimed in a
127 number of stages, was formerly protected by a sea wall and drained into the surrounding marsh
128 through a small sluice gate. To compensate for intertidal habitat loss elsewhere and reduce
129 expenditure on unnecessarily maintaining flood defences of grazing land, Natural Resources Wales
130 opted to stop maintaining the seawall. The site was naturally breached during a storm in August
131 2014, creating a new macrotidal semi-diurnal intertidal system in the approximately 383,000 m² of
132 previously defended grazing land. Consequently, no engineering or design works were performed
133 prior to site breaching.

134

135 **2.2 Spatial variability in the accretion and erosion of sediment**

136

137 2.2.1 sUAS image acquisition

138

139 To assess the spatial variability in sediment accretion and the resulting morphology and topography,
140 an eBee Plus Real-Time Kinematic (RTK) fixed-wing small-unmanned aerial system (sUAS) was used
141 to collect repeat aerial imagery. An initial survey was conducted on 10th March 2015, commissioned
142 by Natural Resources Wales and carried out by Future Aerial Innovations on behalf JBA Consulting. In
143 the 2015 survey, 655 images were collected at a pixel resolution of 3.9 cm / pixel. A second survey
144 was conducted by the authors (also commissioned by Natural Resources Wales) on 3rd July 2019.
145 Flight lines were completed on a grid pattern with an 80% lateral and longitudinal image overlap,
146 and a total of 1047 images captured. Such large overlap values were selected to facilitate increased

147 pixel matching and optimal orthomosaic production; analysis indicated an overlap of over 5+ images
148 for every pixel, and an average of 950 matched 2D key points between image pairs. Multiple flights
149 were flown at 90 m altitude and provided imagery at a pixel resolution of 2.2 cm / pixel. For the
150 purpose of model accuracy, six ground control points (GCPs) were recorded using differential global
151 positioning system (dGPS); measurements taken by a Leica AS19 GNSS antenna, a Leica Viva GS10
152 GPS receiver and a Leica CS15 controller. Raw GPS measurements were imported into Leica Geo
153 Office (version 8.3). Network Receiver Independent Exchange Format (RINEX) correction data were
154 obtained from Leica Smart Net UK & Ireland (http://uk.smartnet-eu.com/rinex-download_148.htm),
155 and used for post processing of eBee Plus flight data and to correct the raw GPS data. Leica Geo
156 Office reported the positional quality (XYZ) for all dGPS points as <0.02 m. In addition to the GCPs,
157 nine independent check points were collected using dGPS to act as an assessment of model quality
158 (see Supplementary Material for the sUAS properties used in this study).

159 2.2.2 sUAS image processing and morphological analysis

160

161 Dense point clouds were produced from optimised camera locations using mild-depth filtering to
162 ensure small and important details were preserved using Pix4D mapper (version 4.2.27). The 2019
163 orthophotograph and DSM were compared to the previous survey (Future Aerial Innovations on
164 behalf JBA Consulting) taken in 2015 in ArcMap (version 10.5.1). DSMs of Difference (DoD) analysis
165 was performed to compare differences between the two modelled surfaces. It is important to
166 consider the uncertainties and potential error propagation when comparing two different DSMs.
167 Therefore, a specified level of detection (LoD) was applied, with any changes smaller than the LoD
168 omitted from the analysis (James et al., 2017). The LoD was defined as:

$$169 \text{LoD} = \pm t (\sigma_{z1}^2 + \sigma_{z2}^2)^{1/2} \quad [\text{Equation 1}]$$

170 where σ_{z1} and σ_{z2} are measures of the vertical error of the two DSMs (Lane et al., 2003), in this case
171 the vertical standard deviations of error, and t is the required level of confidence (95 % used here).

172 Whilst comparing DSM may introduce error due to the inclusion of vegetation, the vegetated area of
173 the site has been colonised by species with a low 'canopy' height such *Salicornia sp.*, *Puccinellia*
174 *maritima*, and *Suaeda maritima*. Consequently, any error introduced is likely to be within the error
175 of the elevation reconstruction (Hladik and Alber, 2012) particularly once the LoD has been applied,
176 which in this instance was calculated to be ± 15 cm.

177

178 Morphological changes were assessed through analysis of the rugosity, an assessment of the surface
179 heterogeneity, derived from the standard deviation of the elevation in a 3 x 3 pixel moving window
180 (Lawrence et al., 2018). Prior to analysis of the 2019 DSM, which originally had a higher pixel
181 resolution, the model was aggregated to coarsen the resolution in order to ensure consistency
182 between the two models. Stream order analysis (Strahler, 1957) was conducted to evaluate the
183 development of the sites drainage network morphology, following the calculation of the flow
184 direction and accumulation, and visually confirmed through a comparison with the orthophotograph
185 (Dale et al., 2020). The difference in total number of creeks in each order between the two surveys
186 was assessed using a Pearson Chi² test. In addition, differences in creek length between the two
187 surveys were assessed for each order using a Mann-Whitney U test as data were not normally
188 distributed (assessed via a quantile-quantile plot), with the median, maximum, minimum, and total
189 creek length also calculated for each order. Analysis was conducted using ArcMap (version 10.5.1)
190 and Minitab (version 19).

191

192 **2.3 Hydrodynamics, suspended sediment concentration and patterns of** 193 **sedimentation**

194

195 To assess the supply and movement of sediment, YSI EXO2 Sondes fitted with conductivity,
196 temperature, depth and turbidity probes were deployed on scaffolding rigs over two spring tidal
197 cycles between 13th and 14th June 2018. Measurements were logged every 10 seconds from an area
198 of colonising saltmarsh and a mudflat environment, 0.39 m lower in elevation than the saltmarsh,
199 and adjacent to the main drainage channels (Figure 1). The Sondes were deployed at 2.75 mOD
200 (Ordnance Datum Newlyn) at the saltmarsh site and 2.73 mOD at the mudflat site. Turbidity probes
201 were calibrated for SSC in the laboratory using filtered water samples taken *in situ*. To measure the
202 pattern of sediment accretion and erosion over a typical tidal cycle at the mudflat site, high
203 frequency bed elevation measurements were taken over the same period using an NKE ALTUS
204 altimeter system. The altimeter consists of a 2 MHz acoustic transducer, supported above the
205 sediment surface on a tripod, which measures the time required for the acoustic signal to return to
206 the transducer from the sediment surface (Jestin et al., 1998), and was also set to measure every 10
207 seconds. Given that the site is fetch and depth limited, and wind levels were low during the
208 measurement period, the impact of wave activity on the deposition and re-suspension of sediment
209 was presumed to be negligible.

210

211 **2.4 Sub-surface geochemistry and preservation of the terrestrial surface**

212

213 Sediment cores were collected from both the saltmarsh site and the mudflat site at Cwm Ivy Marsh
214 for analysis of the sub-surface geochemical profiles and the preservation of the terrestrial surface
215 following site breaching and the accretion of intertidal sediment. Following extraction, samples were
216 wrapped in film, transported back to the University of Brighton Geochemistry Laboratory, and
217 refrigerated at 3.6 °C until analysis. Each core was logged and divided into 2 cm increments to
218 measure a variety of sediment physicochemical characteristics. Specifically, the moisture content,
219 organic content, particle grain size, and a suite of elements (Al, Fe, Mn, S, Ca and Na) were assessed,

220 selected as these parameters have been used at sites such as Orplands Farm (e.g. Spencer et al.,
221 2008), Medmerry (Dale et al., 2019) and Pagham Harbour (Cundy et al., 2002) to identify the
222 terrestrial surface. Moisture content was measured following drying at 105 °C for 48 hours and
223 calculated as the percentage weight loss. Loss of ignition, measured via combustion at 450 °C for six
224 hours, was used as a proxy for organic matter. Particle grain size distribution was analysed using a
225 Malvern Instruments Mastersizer Hydro 2000G Laser Diffraction Particle Size Analyser following
226 treatment in hydrogen peroxide to remove organic matter and dispersion with sodium
227 hexametaphosphate on a rotary shaker at 300 rpm for 2 hours to facilitate disaggregation. For each
228 sample, three replicates were measured for all parameters.

229

230 To support identification of the terrestrial surface, the geochemical composition of the samples was
231 examined. Samples were digested in aqua-regia (1:3 molar ratio of HCl:HNO₃) for three hours in a
232 dry heat block at 80 °C. Samples were filtered through a 0.2 µm syringe filter before dilution in
233 distilled water at 1:10. Samples were analysed for a suit of elements using a Perkin Elmer Optima
234 2100 DV ICP-OES. Samples were analysed alongside the Mess-4 Marine Sediment Certified
235 Reference Material (National Research Council Canada) and process blanks to assess the accuracy of
236 extraction. Recovery values were generally within ± 20 % (see Supplementary Material) and process
237 blanks were below the detection limits. Repeat samples were run in triplicate every 10 samples and
238 were typically within ±10 % throughout.

239

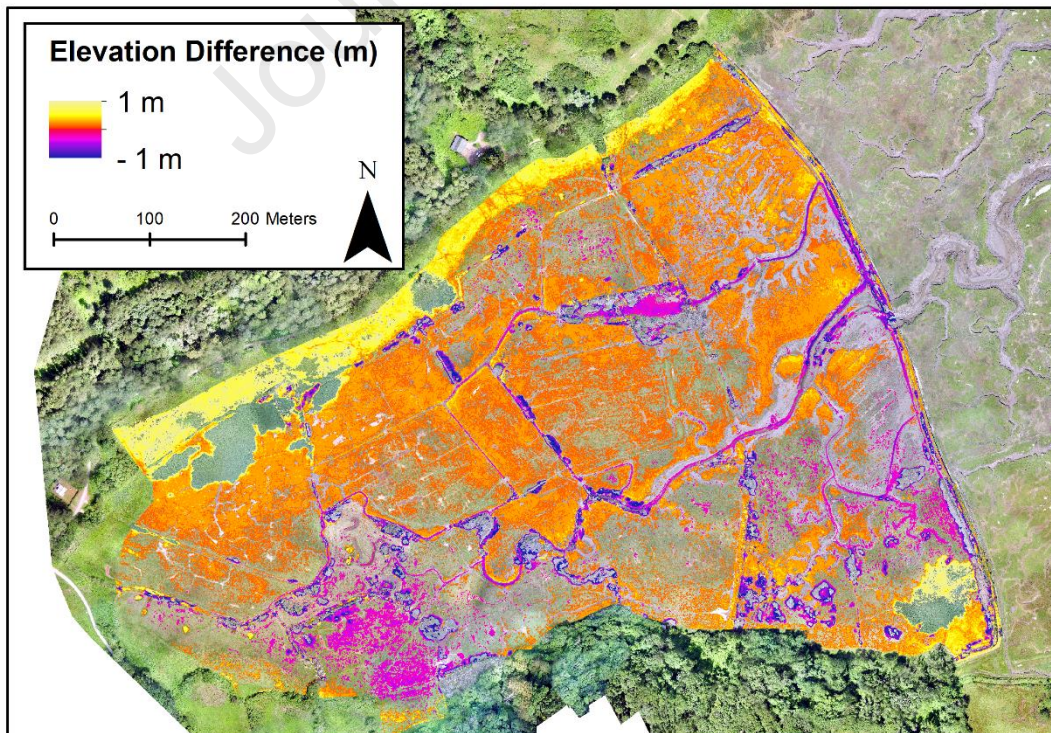
240 **3 Results**

241

242 **3.1 Morphological Development**

243

244 Analysis of the two small-Unmanned Aerial System (sUAS) topographic surveys showed that, over
245 the four-year period, 55.24 % of the 383,000 m² new intertidal area experienced a change in
246 elevation above the level of detection (LoD). Of this area, 22 % (12 % of the entire site) experienced
247 erosion, with sediment accreting in the other 78 % (43 % of the entire site). Erosion was limited to
248 the areas around the main channels running through the site, apart from in the south-western
249 corner of the site where the surface elevation decreased by between 0.2 and 0.3 m between the
250 surveys (Figure 2). The majority of the accretion above the LoD occurred through the centre of the
251 site, to the north of the main channel. Between 15 and 30 cm of sediment was accreted in these
252 areas, giving an average annual accretion rate of 3.75 to 7.5 cm / year. Along the northern side of
253 the site a larger increase in surface elevation of approximately 50 cm was detected. However, given
254 the distance from the main creek network, the relatively high elevation, and the comparably large
255 change in elevation, this area may well consist of transitional or freshwater vegetation; with this
256 change reflective of vegetation growth rather than the accretion of sediment (e.g. Enwright et al.,
257 2018).

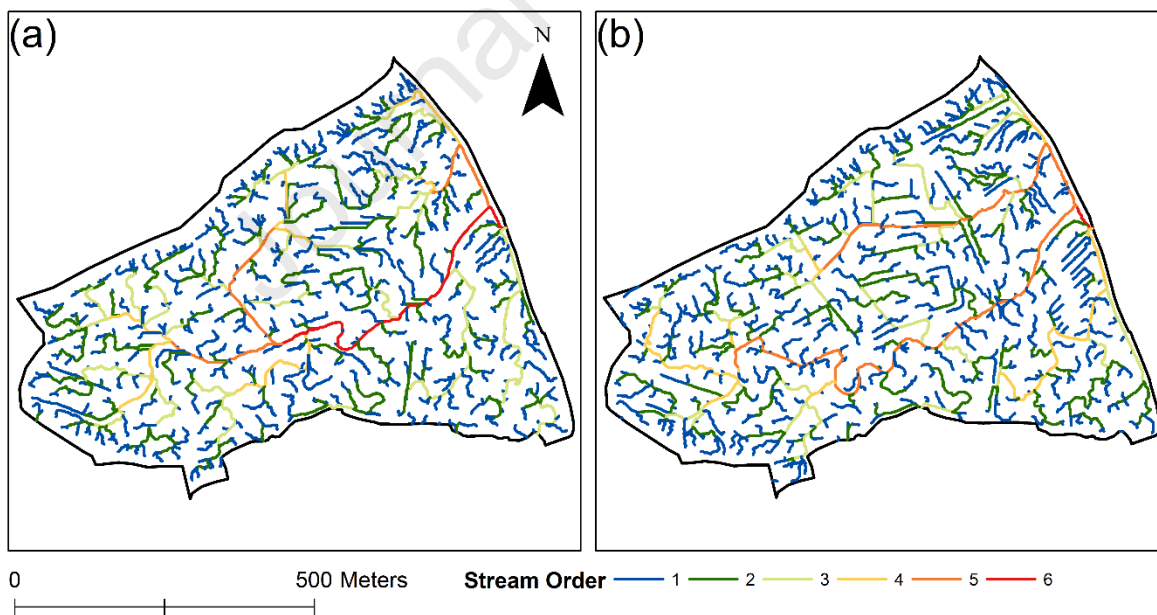


258

259 Figure 2: DSM of Difference (DoD) analysis of the change in elevation between the 2015 and 2019
260 sUAS surveys at Cwm Ivy Marsh, Wales.

261

262 Analysis of the resulting morphological change indicated that the topography within the site became
263 less variable between the two surveys, with the rugosity decreasing from 0.034 to 0.029. Strahler
264 stream order analysis (Figure 3) detected 1047 creeks in 2015 and 1007 creeks in 2019, categorised
265 into six orders. Pearson χ^2 analysis indicated a significant difference ($\chi^2 = 39.95$, $p < 0.01$) in the
266 number of creeks in each order between the two surveys, with fewer lower order and increased
267 higher order creeks being detected in 2019 (Table 2). However, only first order creeks were found to
268 be significantly different in length ($p < 0.01$), with differences in total length due to changes in the
269 number rather than characteristics of the creeks themselves.



270

271 Figure 3: Strahler Stream Order analysis of the creek networks in Cwm Ivy Marsh, Wales in (a) 2015
272 and (b) 2019.

273

274 Table 2: Number of creeks and median, maximum, minimum and total creek length (m) for each
 275 order determined by Strahler Stream Order analysis of the 2015 and 2019 digital surface models
 276 from Cwm Ivy Marsh, Wales.

		First Order	Second Order	Third Order	Fourth Order	Fifth Order	Sixth Order
Number of Creeks	2015	531	278	131	52	32	23
	2019	511	247	108	58	80	3
Median Length (m)	2015	14.30	15.48	17.46	13.35	16.71	24.30
	2019	16.24	16.76	18.60	16.16	15.97	12.79
Maximum Length (m)	2015	111.87	110.80	111.63	95.06	85.29	103.50
	2019	80.33	148.33	75.48	97.61	98.12	37.78
Minimum Length (m)	2015	0.30	0.28	0.28	0.28	0.28	1.28
	2019	0.20	0.28	0.28	0.28	1.57	1.80
Total Length (m)	2015	10168.07	5782.77	2916.36	966.03	685.35	562.24
	2019	11018.47	5403.70	2255.97	1153.20	1554.26	14.59

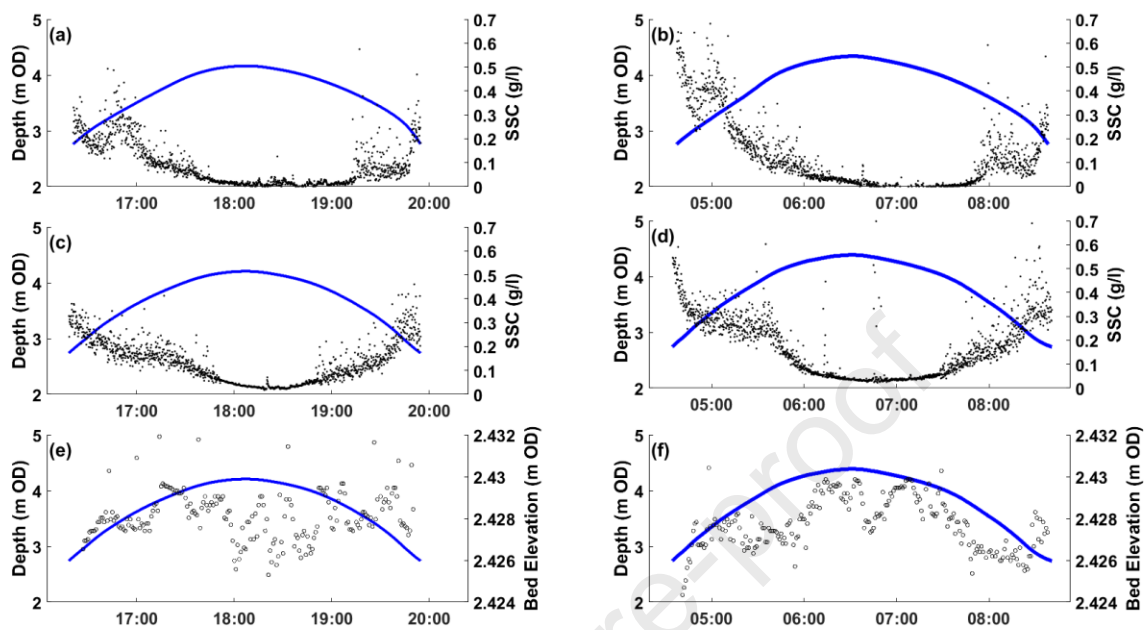
277

278 3.2 Patterns of sedimentation

279

280 The maximum recorded water depth was 4.34 m OD at the saltmarsh site and 4.39 m OD at the
 281 mudflat site, with the water level falling below the sensor during low water at both sites. Peaks in
 282 the SSC (Figure 4) occurred at the onset of the flood tide and towards the end of the ebb tide at both
 283 sites when, typically, the current velocity would be at a maxima; suggesting both the landward and
 284 seaward movement of sediment. Average SSCs per tidal phase were marginally greater during the
 285 flood tide than the ebb at both the saltmarsh site (Tide 1: 0.12 g/l vs 0.06 g/l, Tide 2: 0.19 g/l vs 0.08
 286 g/l) and the mudflat site (Tide 1: 0.15 vs 0.11 g/l, Tide 2: 0.21 vs 0.14 g/l). As no current velocity
 287 measurements were collected during this study the sediment flux and net direction of sediment
 288 transport could not be calculated. However, some variability was detected in the SSC at the
 289 saltmarsh site during the flood tide, which is probably related to the flooding pattern and drainage
 290 system characteristics within the site. Changes in bed elevation at the mudflat site (Figure 4e-f)

291 followed a pattern of sedimentation then erosion during both the flood and ebb tidal phases, with a
 292 net increase in bed elevation of 0.1 cm during Tide 1 and 0.3 cm during Tide 2.



293

294 Figure 4: Changes in depth (blue solid line) and suspended sediment concentration (SSC, dots) for
 295 Tide 1 (left side) and Tide 2 (right side) at (a-b) the saltmarsh site (c-d) the mudflat site, and changes
 296 in bed elevation (averaged every minute for presentation purposes, circles) at (e-f) the mudflat site
 297 at Cwm Ivy Marsh, Wales. The time period for sampling (24H) is indicated by the x-axis.

298

299 3.3 Subsurface structure and geochemistry

300

301 At both sites clear vertical zonation was exhibited visually, with the cores divided into a lower
 302 terrestrial unit and an upper post-breach intertidal unit dating from August 2014. At both sites, this
 303 horizon occurred at 12 cm depth. The upper section of the 28 cm core retrieved from the saltmarsh
 304 site consisted of compact, grey, clay rich sediment with vertical root material. Following a sharp
 305 boundary at the horizon between the two units, the lower section of the core was more friable with

306 evidence of red mottling and organic root material. At the mudflat site, where a 38 cm core was
307 retrieved, the upper 12 cm consisted of dark, black clay and silt rich sediment. Below a sharp
308 boundary at the horizon, the lower terrestrial unit was more friable and contained a higher
309 proportion of silt and sand. A large amount of root and organic material was found at, and below,
310 the horizon.

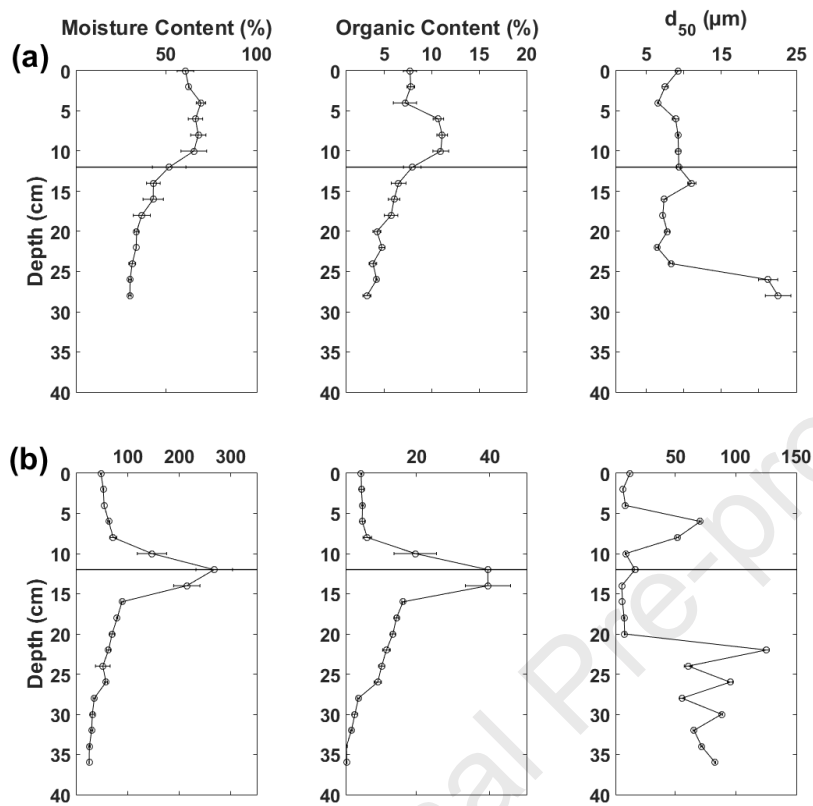
311

312 Confirmation of the location of the pre-breach terrestrial surface was assessed through analysis of
313 the sub-surface physicochemical profiles. At the saltmarsh site (Figure 5a), moisture content and loss
314 on ignition decreased with depth. Both of these parameters were greater at the mudflat site (Figure
315 5b), where a similar trend was observed with both parameters peaking at the terrestrial / intertidal
316 sub-surface horizon. Median grain size was relatively similar at both sites in the intertidal units,
317 although more variability was observed at the mudflat site. In the terrestrial sections, median grain
318 size increased at 26 cm at the saltmarsh site and 22 cm at the mudflat site, possibly the result of
319 aeolian sediment transport from sand dunes located to the north and northwest of the site.

320

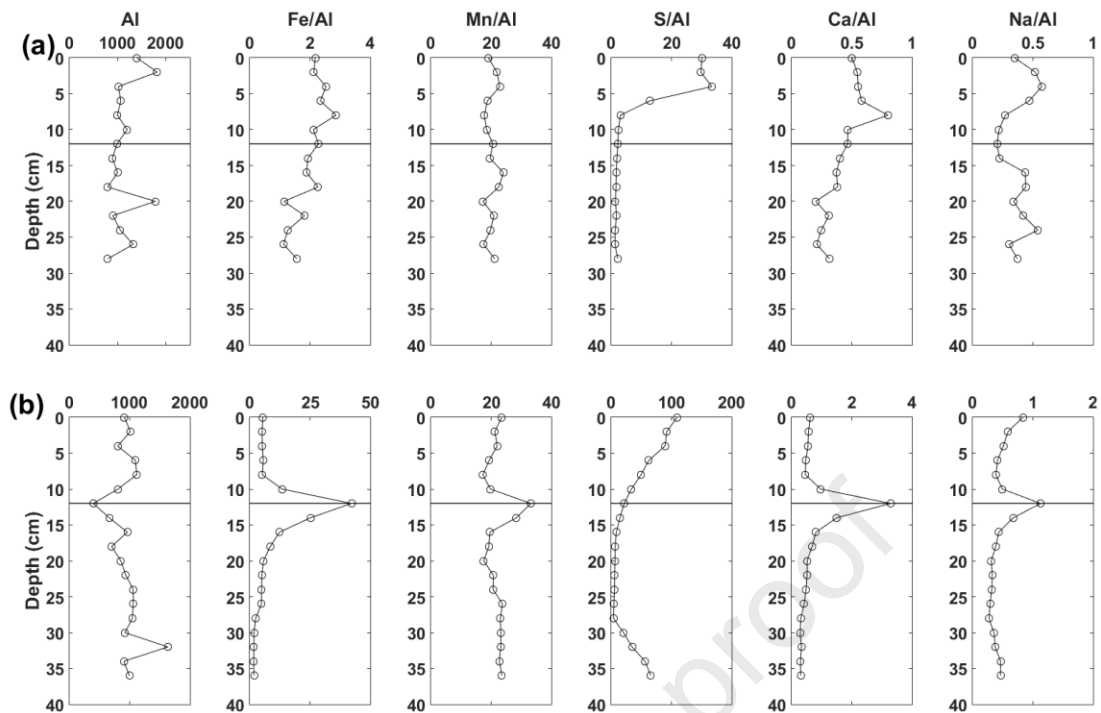
321 Figure 6 presents the major element data (Al, Fe, Mn, S, Ca and Na) for both sites. As grain size
322 varied with depth, concentrations of Fe, Mn, S, Ca and Na have been geochemically normalised to Al
323 (after Spencer et al., 2008). The diagenetic enhancement of Fe and Mn in oxic saltmarsh sediments
324 has been recognised and described in depth elsewhere (e.g. Cundy and Croudace, 1995; Spencer et
325 al., 2003; Zwolsman et al., 1993). Concentrations of Fe and Mn fluctuated throughout the sediment
326 at the saltmarsh site, with no major peaks or trends. This, along with the evidence of red mottling
327 caused by the presence of Fe-oxyhydroxides (Zwolsman et al., 1993) indicates a fluctuating water
328 table, and periodic shifts from oxidising to reducing conditions during tidal inundation. The
329 saltmarsh site showed a depletion of S except in the upper 6 cm, probably due to the introduction,

330 percolation and evaporation of sea water, rather than the bacterial reduction of sulphate. Both Ca
 331 and Na fluctuated with Ca, decreasing slightly with depth.



332

333 Figure 5: Moisture content, loss on ignition and median grain size (d_{50}) with depth ($n = 3$) for (a) the
 334 saltmarsh site and (b) the mudflat site at Cwm Ivy Marsh, Wales. The solid line marks the position of
 335 the solid boundary between the two units.



336

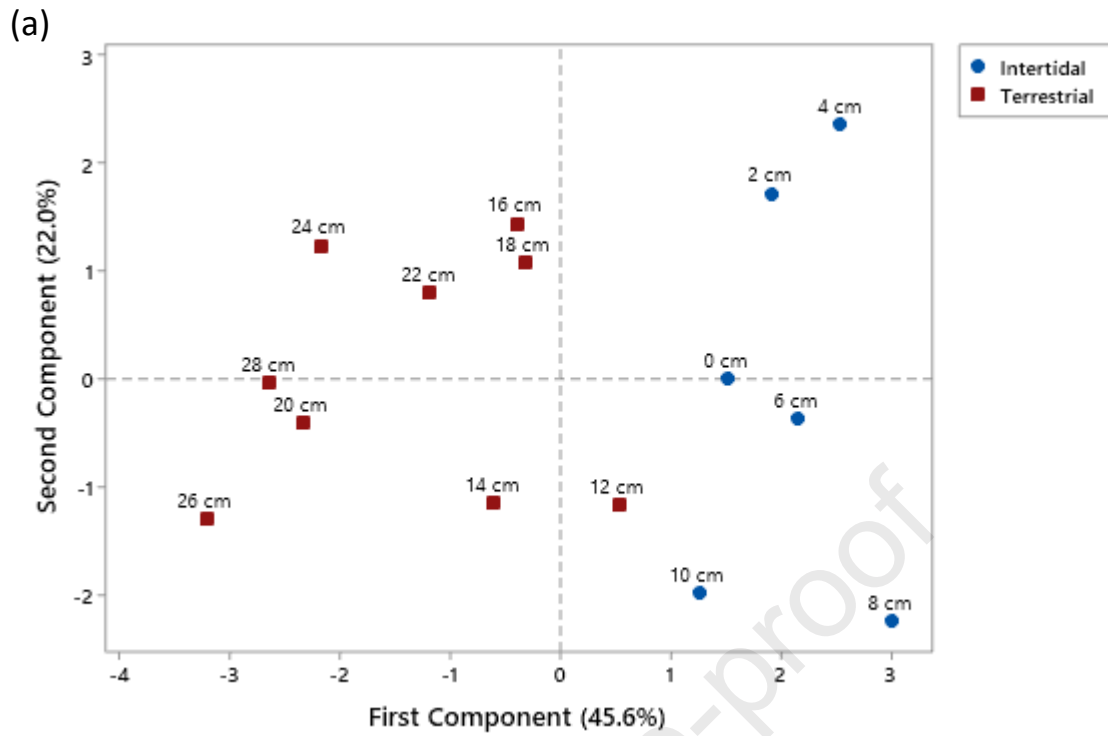
337 Figure 6: Variations in Al, Fe, Mn, S, Ca and Na with depth ($n = 3$) for (a) the saltmarsh site and (b)
 338 the mudflat site at Cwm Ivy Marsh, Wales. The solid line marks the position of the solid boundary
 339 between the two units.

340

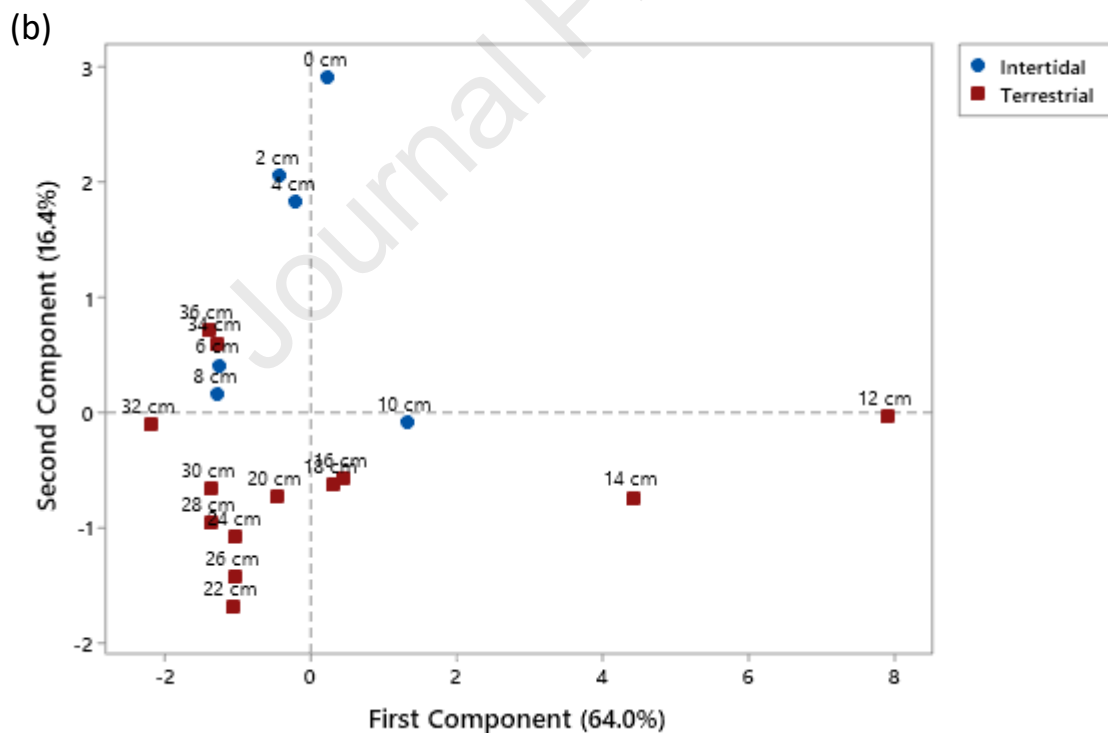
341 At the mudflat site a greater concentration of S was found, suggesting conditions are permanently
 342 reducing and the supply of oxygen limited. A peak in Fe and Mn concentration was found at the
 343 terrestrial / intertidal boundary, indicative of the remobilisation of Fe and Mn from the reducing
 344 sediments. This may well be caused by poor hydrological connectivity resulting in water being
 345 unable to penetrate through the terrestrial surface and flowing along the interface between the two
 346 units, explaining the high moisture content found at this depth. Evidence of vertical inhabitation of
 347 saline water is supported by peaks in the Ca and Na concentrations at the interface between the two
 348 units.

349

350 Further confirmation of the location of the pre-breach terrestrial surface is possible through
351 Principal Component Analysis (PCA) of the sediment physicochemical properties. PCA is a technique
352 used to reduce the dimensionality of data through the calculation of a series of new variables, or
353 principle components, through linear combinations of the original parameters (Reid and Spencer,
354 2009). This multivariate technique has previously been used successfully elsewhere in coastal
355 sediments to (partially) discriminate physicochemical datasets (e.g. Cundy et al., 2006; Dale et al.,
356 2019), and was used here to group different depths based on their variability in sediment
357 physicochemical properties. Results indicated that, at the saltmarsh site (Figure 7a), the first
358 component accounted for the greatest variability (PC1 = 46%, Eigenvalue = 4.10) and described a
359 clear separation in the sediment physicochemical properties between identified intertidal and
360 terrestrial units (Figure 7a). Limited discrimination was found in the subsequent principal
361 components (e.g. PC2 = 22%, Eigenvalue = 1.98). Conversely, the mudflat site (Figure 7b) showed the
362 clearest separation between terrestrial and intertidal sediment physicochemical properties through
363 the second component scores (PC1 = 64%, Eigenvalue = 5.76; PC2 = 16%, Eigenvalue = 1.47). The first
364 component showed the greatest variability was between the samples at 12 and 14 cm depth, the
365 horizon between the intertidal and terrestrial layers, likely to be the result of peaks in the moisture
366 content, organic content and Fe, Mn, Ca and Na.



367



368

369 Figure 7: Principal component analysis for (a) the saltmarsh site and (b) the mudflat site of the
 370 physicochemical properties for different depths at Cwm Ivy Marsh, Wales. Blue circles represent
 371 depths identified visually as being the post-site breaching intertidal unit, and red squares are the

372 terrestrial unit. Collectively, components 1 and 2 accounted for 67.5% of the variability at the
373 saltmarsh site and 80.3% of the variability at the mudflat site.

374

375

376

377 **4 Discussion**

378

379 **4.1 Surface Morphological Evolution**

380

381 Examination of the spatial and temporal pattern of erosion and accretion at Cwm Ivy Marsh,
382 presented via an innovative combination of sUAS derived topographic and morphological,
383 hydrological and geochemical analysis, provides a new insight into the development of newly
384 inundated intertidal wetlands. Evaluation of whole site topographic variability, assessed through
385 analysis of the DSM rugosity, indicated a decrease in surface heterogeneity between the two
386 surveys; and highlights the importance of full-site assessment. Elsewhere, rugosity has been
387 demonstrated to correlate positively with number of creeks (Lawrence et al., 2018) with analysis of
388 the creek network at Cwm Ivy Marsh corroborating this finding; the number of creeks also decreased
389 between the two surveys. These findings are also similar to those of Dale et al. (2020) who observed
390 a reduction in the number of creeks, albeit within a much smaller study area, which the authors
391 associated with an increase in the prominence of some of the channels in terms of site drainage.

392

393 As a non-engineered site, Cwm Ivy Marsh did not experience any artificial channel creation,
394 excavation or re-profiling, which is common practice in large engineered sites (Burgess et al., 2014;
395 Dale et al., 2018b). Previous studies have also identified pre-existing terrestrial features such as relic
396 plough lines as a major influence on creek development in MR sites (Dale et al., 2020; French and
397 Stoddart, 1992). However, the Cwm Ivy site was used predominantly for grazing and is not known to
398 have experienced intensive arable agricultural activity. Nonetheless, the site is still developing a
399 functioning drainage system utilising the pre-existing areas of lower elevation, remnant pre-
400 reclamation creeks and artificial drainage networks. This is evident from the combination of both
401 dendritic channels and straighter channels running parallel to the old sea wall, perpendicular to the
402 direction of higher order creeks, and in some cases away from the breach area. Consequently, these
403 results indicate that, providing some form of drainage systems exist, MR sites are still capable of
404 developing functioning intertidal morphology without the need to extensive site landscaping. The
405 site is also appearing to decrease in topographical variability. This may inhibit the formation of the
406 distinct elevational niches required by saltmarsh plants (Masselink et al., 2017; Sullivan et al., 2017),
407 although further research is required to assess the relationship between saltmarsh coverage,
408 colonisation and morphology in non-engineered MR sites, and restored saltmarshes more widely.

409

410 Analysis of the spatial pattern of accretion and erosion was performed via DoD analysis of the DSMs,
411 recognising the limitations of LoD factors. Results indicated that erosion was limited to the area
412 around the channels with accretion occurring across the majority of site, particularly to the north of
413 the main channel. In these areas sediment accreted at a rate of 3.75 to 7.5 cm / year. This rate of
414 accretion is slightly higher than that calculated through analysis of the accretion above the terrestrial
415 surface recorded in the sediment cores retrieved from Cwm Ivy Marsh, which indicated that an
416 accretion rate of 3 cm / year. However, it is worth to note that 3 cm / year, equivalent to 12 cm of
417 accretion, would have returned a change in elevation below the LoD (± 15 cm) for these surveys.

418 These results highlight the importance for continuing to advance high resolution, site-wide,
419 empirical studies of this nature through a combination of repeat high spatial resolution remote
420 sensing or sUAS approaches, alongside high temporal resolution analysis using equipment such as
421 the ALTUS used in this study.

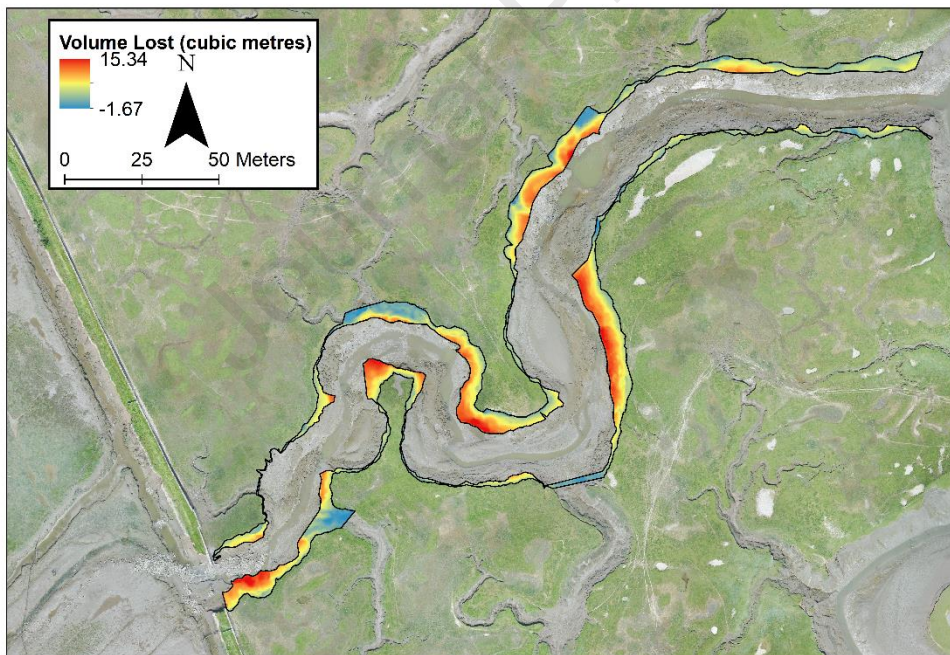
422

423 Sediment was accreted and eroded during both the flood and ebb tides were measured by the
424 ALTUS system deployed at Cwm Ivy Marsh, which differs from the patterns found elsewhere within
425 natural intertidal sites. For example, Deloffre et al. (2007) detected a pattern of accretion during the
426 flood tide and dewatering and erosion during the ebb in the Seine estuaries, which has a similar rate
427 of sediment accumulation to those measures here for Cwm Ivy Marsh. Furthermore, a pattern of
428 sedimentation on the flood tide and stability during the ebb was measured for the Authie estuaries
429 by Deloffre et al. (2007). A similar pattern to the Authie was found at the Medmerry Managed
430 Realignment Site, at a near breach site, by Dale et al. (2017), whilst in the centre of the site the
431 pattern followed a trend of accretion on the flood and erosion on the ebb (Dale et al., 2017; Dale et
432 al., 2018b). However, Cwm Ivy marsh differs from these three sites as, unlike the Seine and the
433 Authie, there is negligible fluvial input and there is a much larger tidal range than Medmerry. This,
434 therefore, highlights the importance of the internal and external hydrodynamics (such as the current
435 velocity, tidal input and fluvial input) on the deposition and accretion of sediment, which in turn
436 influences the physical functioning post-site breaching and morphological evolution of the site.

437

438 The pattern of sedimentation is also determined by the post site breaching supply and internal
439 redistribution of sediment. Peaks in the SSC were observed on the flood and ebb tide at both sites,
440 although the source of the sediment remains unknown. Some of this sediment may be material
441 internally redistributed around the site as the sediment regime adjusts to intertidal conditions.

442 However, previous studies from MR sites in sediment rich estuaries, fronted by natural saltmarshes,
443 have suggested that the transported and accreted sediment has originated from external sources
444 (e.g. Rotman et al., 2008; Symonds and Collins, 2005). Whilst no measurements of the fluxes of SSC
445 were recorded in the breach for this study, it is highly likely that the channel feeding into Cwm Ivy
446 Marsh has been the major source of sediment. An examination of the two orthophotographs and
447 DSMs, collected as part of the sUAS analysis, indicated that from the channel immediately flowing
448 into the site 29392 m³ of sediment were eroded from a 2424 m² area of saltmarsh between March
449 2015 and July 2019 (Figure 8). In addition, the breach has widened from 9.96 m (2015) to 14.79 m
450 (2019) during this time. This erosion and channel widening will have been caused by an increase in
451 discharge and velocity within the channel owing to the increased transfer of water following site
452 breaching, providing a readily available source of sediment to the Cwm Ivy site.



453

454 Figure 8: Volume of sediment lost (m³) per 4 m² pixel from the channel leading into Cwm Ivy Marsh,
455 Wales.

456

457 The previous understanding of the morphological evolution of recently inundated saltmarsh sites is
458 largely derived from theoretical models (e.g. Allen, 2000), which suggest that initially high rates of
459 sedimentation should be expected following site breaching. In addition, some field-based
460 measurements (e.g. Dixon et al., 2008; Virgin et al., 2020) do exist, however most empirical
461 measurements of the morphological development post-site breaching have been calculated from
462 heavily engineered sites, using either sediment cores or traditional remote surveying techniques
463 such as LiDAR or GPS (Chirol et al., 2018; Cundy et al., 2002; Dale et al., 2018a; Lawrence et al., 2018;
464 van Proosdij et al., 2010; Virgin et al., 2020). As a result of the lack of full site, high resolution spatial
465 analysis, combined with specific high-frequency field measurements of the sedimentological
466 processes important morphological changes that are smaller than the surveying resolution are likely
467 to have been missed.

468

469 In addition to limitations resulting from the resolution of previous studies, the evolution of the sites
470 examined in these investigations may have been influenced by site design and landscaping
471 processes. Therefore, the development of these sites may not be representative of the
472 morphological evolution resulting from the introduction of tidal inundation. For example, Dale et al.
473 (2017) measured a similar rate of accretion at the centre of the Medmerry Managed Realignment
474 Site to those measured in this study, regardless of the temporal variability. Conversely, the accretion
475 rates at Cwm Ivy were considerably lower than those observed in an area of lower elevation near
476 the breach at the Medmerry site by Dale et al. (2017). However, these measurements were taken at
477 locations which had been artificially lowered during site construction to encourage a range of
478 intertidal habitat, creating accommodation space for sediment to be accreted. In contrast, no
479 engineering works took place at Cwm Ivy Marsh prior to site breaching, and therefore allows for the
480 rate of accretion to be assessed without the influence of engineering and site landscaping, which is
481 often carried out on the basis that it would enhance site development.

482

483 Further work is required to assess the external and internal sources of sediment, and to determine
484 the areas of deposition, to calculate the changes in sediment volume and the sediment budget as
485 sites develop following the introduction of intertidal inundation. This is particularly the case for non-
486 engineered sites to further the understanding of influence site design and pre-breach landscape
487 have on the functioning and evolution of the sediment regime. This will, in turn, inform analysis of
488 the physical functioning and the morphological evolution of MR sites which has been recognised to
489 differ between MR sites and equivalent natural marshes (Lawrence et al., 2018). Many sites are
490 subject to extensive engineering based on numerically modelled site designs derived simply on the
491 hydroperiod (frequency and duration of inundation) and the elevation. These parameters are often
492 considered equal to parameters such as the aesthetics, and other factors which may not be most
493 suitable for a natural system. For example, Steart Managed Realignment Site was designed with a
494 herringbone channel pattern, rather than a natural dendritic creek network, due to concerns of the
495 safety of cattle grazing the marsh during the rising flood tide (Burgess et al., 2014). As a result, it is
496 possible that the site design and landscaping may hinder the hydrological evolution and physical
497 functioning of engineered MR sites.

498

499 Analysis of non-engineered MR sites will also validate predictions of future non-engineered MR sites
500 (e.g. Krolik-Root et al., 2015), breached following policies no active intervention and the decision to
501 no long maintain defences in selected located. In addition, non-engineered MR sites provide a
502 modern analogue for historically breached sites, such as Pagham Harbour, West Sussex, UK, and
503 locations around the Essex (southeast England) coastline (Cundy et al., 2002; Spencer et al., 2017).
504 These sites have often been identified as natural field laboratories for assessing the potential longer-
505 term outcome for modern day MR sites. Comparisons of the processes in modern engineered and

506 non-engineered MR sites will allow for the evaluation of the suitability of this approach, and validate
507 the use of older naturally breached sites to estimate the evolution of future MR schemes.

508

509

510 **4.2 Evolution of the sediment sub-surface and the preservation of the terrestrial** 511 **surface**

512

513 Analysis of the rate of accretion following site breaching was possible via visual detection of
514 terrestrial surface, and confirmed through PCA of the sediment physicochemical properties. Visual
515 detection of the terrestrial surface has been performed elsewhere at similarly aged sites such as the
516 Medmerry Managed Realignment Site (Dale, 2018), although considerably more intertidal sediment
517 has been accreted at Cwm Ivy Marsh following site breaching. At older accidentally breached and MR
518 sites, including Pagham Harbour and Orplands Farm (Cundy et al., 2002; Spencer et al., 2008), the
519 terrestrial surface could not be detected visually. The interface between the terrestrial and intertidal
520 units could only be identified through analysis of the physicochemical properties, and detailed three-
521 dimensional analysis of the sediment structure (Spencer et al., 2017), highlighting the transient
522 nature of analysis of developing intertidal sites. Nonetheless the findings this study, compared to
523 these observations from elsewhere, indicate that the ability to detect the terrestrial surface is a
524 function of time since intertidal inundation, and not the result of changes to the sediment sub-
525 surface.

526

527 Analysis of the sub-surface geochemical properties at Cwm Ivy Marsh indicate a fluctuating water
528 table in the freely draining sediment of the saltmarsh site. This is consistent with the redox profiles
529 typically found in natural intertidal environments (e.g. Cundy and Croudace, 1995), suggesting that

530 reduced hydrological connectivity and an aquaclude-like horizon, found in other, older MR sites (e.g.
531 Boorman, 1992; Hazelden and Boorman, 2001; Tempest et al., 2015), is not present. As would be
532 expected, anoxic conditions were found at the mudflat site. However, some evidence of the
533 remobilisation of Fe and Mn, potentially caused by an aquaclude horizon, was also found, although
534 given the peak in organic content at this depth the increase in Fe and Mn may also be caused by the
535 decay of freshwater vegetation buried under the accreted sediment (Macleod et al., 1999). Reduced
536 hydrological connectivity has been associated with modifications to the sediment structure due to
537 dewatering and organic matter mineralisation, as a result of the agricultural activity (e.g. Crooks and
538 Pye, 2000; Crooks et al., 2002). Given that the terrestrial land use of Cwm Ivy Marsh was
539 predominantly sheep grazing land, and the site was not subject to any pre-inundation landscaping, it
540 is unlikely to have experienced the same level of disturbance (compaction, collapse of pore-space,
541 construction of artificial drainage features) as other MR sites (Burgess et al., 2014; Spencer et al.,
542 2017). This in turn appears to be allowing for a more natural intertidal system to develop,
543 maximising the potential for ecosystem service provision, such as habitats and nursery grounds for
544 fish species.

545

546 **5 Conclusion**

547

548 High spatial resolution topographic models, innovatively combined with short-term high frequency
549 hydrological, bed elevation and sediment core data have been examined to assess the morphological
550 evolution of a non-engineered MR site. During the flood tide SSC decreased, and increased during
551 the ebb, suggesting sediment is transported landwards during the incoming tide and flushed
552 seaward during the outgoing tide. Bed elevation increased and decreased during both the flood and
553 ebb tides, with this pattern resulting in a sedimentation rate of 3 to 7.5 cm / year. Following four

554 years of intertidal inundation the site has developed morphologically, yet the terrestrial surface
555 could still be detected both visibly and via analysis of the physicochemical properties.

556

557 Cwm Ivy Marsh had previously been used for sheep grazing, and was not subjected to intensive
558 agricultural activity or extensive site design and landscaping prior to tidal inundation. Nonetheless,
559 as the site has developed pre-existing features such as reclamation drainage channels and areas of
560 lower elevation have contributed to site development. This highlights the importance of evaluating,
561 and utilising where appropriate, the on-site terrestrial morphology during site design and in
562 predictions of site evaluation. Furthermore, whilst differences between the terrestrial and intertidal
563 sediment units could be detected, particularly following PCA of the sediment properties at different
564 depths, the geochemical composition of the sediment subsurface followed the trends expected in a
565 natural intertidal environment. This contrasts with analysis of other (older) MR sites where changes
566 in the sediment structure have been detected as a result of the former agricultural land use, which
567 has been recognised to lower hydrological connectivity leading to reduced biodiversity and
568 abundance of key saltmarsh species.

569

570 This paper addresses this shortage of baseline data via a novel combination of high frequency and
571 high spatial resolution datasets. Further analysis of sites like Cwm Ivy Marsh, including longer-term
572 analysis of the erosion, transportation, deposition and consolidation of sediment, is required to
573 further the understanding of evolution of MR sites without the influence of these processes. This can
574 then inform coastal managers and decision makers in terms of the location and design of future MR
575 sites in order to reduce the influence of alterations to the sediment structure and to evaluate the
576 need for costly engineering works prior to site breaching. This will maximise the extent to which the

577 physical functioning of MR sites represents a natural intertidal environment, increasing the delivery
578 of key ecosystem services provided by these sites.

579

580 **Acknowledgments**

581 The authors would like to thank: Shari Gallop and two other anonymous reviewers for their detailed
582 and supportive comments; Magda Grove and Matthew Leake (both University of Brighton) for their
583 assistance during field work; Corrinne Benbow (National Trust) and James Moon (Natural Resources
584 Wales) for their support, guidance and for providing accommodation during field campaigns; Natural
585 Resources Wales for granting access to previous survey data carried out by Future Aerial Innovations
586 on behalf JBA Consulting. Financial support for this research was provided by Natural Resources
587 Wales and the School of Environment and Technology, University of Brighton.

588

589 **References**

590

- 591 Adam, P., 2002. Saltmarshes in a time of change. *Environmental Conservation* 29, 39-61.
- 592 Allen, J.R.L., 2000. Morphodynamics of Holocene salt marshes: a review sketch from the Atlantic and
593 Southern North Sea coasts of Europe. *Quaternary Science Reviews* 19, 1155-1231.
- 594 Barbier, E.B., Hacker, S.D., Kennedy, C., Koch, E.W., Stier, A.C., Silliman, B.R., 2011. The value of
595 estuarine and coastal ecosystem services. *Ecological Monographs* 81, 169-193.
- 596 Boorman, L., 1992. The environmental consequences of climatic change on British salt marsh
597 vegetation. *Wetlands Ecology and Management* 2, 11-21.
- 598 Burgess, K., Pontee, N., Wilson, T., Lee, S.C., Cox, R., 2014. Steart coastal management project:
599 engineering challenges in a hyper-tidal environment, *From Sea to Shore—Meeting the Challenges of*
600 *the Sea: (Coasts, Marine Structures and Breakwaters 2013)*. ICE Publishing, pp. 665-674.
- 601 Callaway, J.C., 2005. The Challenge of Restoring Functioning Salt Marsh Ecosystem. *J Coastal Res*, 24-
602 36.
- 603 Chirol, C., Haigh, I.D., Pontee, N., Thompson, C.E., Gallop, S.L., 2018. Parametrizing tidal creek
604 morphology in mature saltmarshes using semi-automated extraction from lidar. *Remote Sensing of*
605 *Environment* 209, 291-311.
- 606 Crooks, S., Pye, K., 2000. Sedimentological controls on the erosion and morphology of saltmarshes:
607 implications for flood defence and habitat recreation, in: Pye, K., Allen, J.R.L. (Eds.), *Coastal and*
608 *Estuarine Environments: Sedimentology, Geomorphology and Geoarchaeology*, pp. 207-222.
- 609 Crooks, S., Schutten, J., Sheern, G.D., Pye, K., Davy, A.J., 2002. Drainage and elevation as factors in
610 the restoration of salt marsh in Britain. *Restoration Ecology* 10, 591-602.
- 611 Cundy, A.B., Croudace, I.W., 1995. Sedimentary and geochemical variations in a salt-marsh mud flat
612 environment from the mesotidal Hamble estuary, southern England. *Marine Chemistry* 51, 115-132.
- 613 Cundy, A.B., Long, A.J., Hill, C.T., Spencer, C., Croudace, I.W., 2002. Sedimentary response of Pagham
614 Harbour, southern England to barrier breaching in AD 1910. *Geomorphology* 46, 163-176.
- 615 Cundy, A.B., Sprague, D., Hopkinson, L., Maroukian, H., Gaki-Papanastassiou, K., Papanastassiou, D.,
616 Frogley, M.R., 2006. Geochemical and stratigraphic indicators of late Holocene coastal evolution in
617 the Gythio area, southern Peloponnese, Greece. *Marine Geology* 230, 161-177.
- 618 Dale, J., 2018. The evolution of the sediment regime in a large open coast managed realignment site:
619 a case study of the Medmerry Managed Realignment Site. University of Brighton.
- 620 Dale, J., Burgess, H.M., Burnside, N.G., Kilkie, P., Nash, D.J., Cundy, A.B., 2018a. The evolution of
621 embryonic creek systems in a recently inundated large open coast managed realignment site.
622 *Anthropocene Coasts* 1, 16-33.
- 623 Dale, J., Burgess, H.M., Cundy, A.B., 2017. Sedimentation rhythms and hydrodynamics in two
624 engineered environments in an open coast managed realignment site. *Marine Geology* 383, 120-
625 131.
- 626 Dale, J., Burgess, H.M., Nash, D.J., Cundy, A.B., 2018b. Hydrodynamics and sedimentary processes in
627 the main drainage channel of a large open coast managed realignment site. *Estuarine, Coastal and*
628 *Shelf Science* 215, 100-111.
- 629 Dale, J., Burnside, N.G., Strong, C.J., Burgess, H.M., 2020. The use of small-Unmanned Aerial Systems
630 for high resolution analysis for intertidal wetland restoration schemes. *Ecological Engineering* 143.
- 631 Dale, J., Cundy, A.B., Spencer, K.L., Carr, S.J., Croudace, I.W., Burgess, H.M., Nash, D.J., 2019.
632 Sediment structure and physicochemical changes following tidal inundation at a large open coast
633 managed realignment site. *Science of The Total Environment* 660, 1419-1432.
- 634 Deloffre, J., Verney, R., Lafite, R., Lesueur, P., Lesourd, S., Cundy, A.B., 2007. Sedimentation on
635 intertidal mudflats in the lower part of macrotidal estuaries: Sedimentation rhythms and their
636 preservation. *Marine Geology* 241, 19-32.

- 637 Dixon, M., Morris, R.K.A., Scott, C.R., Birchenough, A., Colclough, S., 2008. Managed realignment -
 638 lessons from Wallasea, UK. *Proceedings of the Institution of Civil Engineers-Maritime Engineering*
 639 161, 61-71.
- 640 Enwright, N.M., Wang, L., Borchert, S.M., Day, R.H., Feher, L.C., Osland, M.J., 2018. The Impact of
 641 Lidar Elevation Uncertainty on Mapping Intertidal Habitats on Barrier Islands. *Remote Sensing* 10.
- 642 French, J.R., Stoddart, D.R., 1992. Hydrodynamics of salt marsh creek systems: Implications for
 643 marsh morphological development and material exchange. *Earth Surface Processes and Landforms*
 644 17, 235-252.
- 645 French, P.W., 2006. Managed realignment - The developing story of a comparatively new approach
 646 to soft engineering. *Estuarine Coastal and Shelf Science* 67, 409-423.
- 647 Garbutt, R.A., Reading, C.J., Wolters, M., Gray, A.J., Rothery, P., 2006. Monitoring the development
 648 of intertidal habitats on former agricultural land after the managed realignment of coastal defences
 649 at Tollesbury, Essex, UK. *Marine Pollution Bulletin* 53, 155-164.
- 650 Hazelden, J., Boorman, L.A., 2001. Soils and 'managed retreat' in South East England. *Soil Use and*
 651 *Management* 17, 150-154.
- 652 Hladik, C., Alber, M., 2012. Accuracy assessment and correction of a LIDAR-derived salt marsh digital
 653 elevation model. *Remote Sensing of Environment* 121, 224-235.
- 654 Howe, A.J., Rodriguez, J.F., Spencer, J., MacFarlane, G.R., Saintilan, N., 2010. Response of estuarine
 655 wetlands to reinstatement of tidal flows. *Marine and Freshwater Research* 61, 702-713.
- 656 James, M.R., Robson, S., Smith, M.W., 2017. 3-D uncertainty-based topographic change detection
 657 with structure-from-motion photogrammetry: precision maps for ground control and directly
 658 georeferenced surveys. *Earth Surface Processes and Landforms* 42, 1769-1788.
- 659 Jestin, H., Bassoullet, P., Le Hir, P., L'Yavanc, J., Degres, Y., 1998. Development of ALTUS, a high
 660 frequency acoustic submersible recording altimeter to accurately monitor bed elevation and
 661 quantify deposition or erosion of sediments, *Oceans'98 - Conference Proceedings, Vols 1-3. IEEE,*
 662 *New York, pp. 189-194.*
- 663 Kroluk-Root, C., Stansbury, D.L., Burnside, N.G., 2015. Effective LiDAR-based modelling and
 664 visualisation of managed retreat scenarios for coastal planning: An example from the southern UK.
 665 *Ocean & Coastal Management* 114, 164-174.
- 666 Lane, S.N., Westaway, R.M., Hicks, D.M., 2003. Estimation of erosion and deposition volumes in a
 667 large, gravel-bed, braided river using synoptic remote sensing. *Earth Surface Processes and*
 668 *Landforms* 28, 249-271.
- 669 Lawrence, P.J., Smith, G.R., Sullivan, M.J.P., Mossman, H.L., 2018. Restored saltmarshes lack the
 670 topographic diversity found in natural habitat. *Ecological Engineering* 115, 58-66.
- 671 Macleod, C.L., Scrimshaw, M.D., Emmerson, R.H.C., Chang, Y.H., Lester, J.N., 1999. Geochemical
 672 changes in metal and nutrient loading at Orplands Farm Managed Retreat site, Essex, UK (April 1995-
 673 1997). *Marine Pollution Bulletin* 38, 1115-1125.
- 674 Masselink, G., Hanley, M.E., Halwyn, A.C., Blake, W., Kingston, K., Newton, T., Williams, M., 2017.
 675 Evaluation of salt marsh restoration by means of self-regulating tidal gate – Avon estuary, South
 676 Devon, UK. *Ecological Engineering* 106, Part A, 174-190.
- 677 Mazik, K., Musk, W., Dawes, O., Solyanko, K., Brown, S., Mander, L., Elliott, M., 2010. Managed
 678 realignment as compensation for the loss of intertidal mudflat: A short term solution to a long term
 679 problem? *Estuarine, Coastal and Shelf Science* 90, 11-20.
- 680 Moller, I., Kudella, M., Rupprecht, F., Spencer, T., Paul, M., van Wesenbeeck, B.K., Wolters, G.,
 681 Jensen, K., Bouma, T.J., Miranda-Lange, M., Schimmels, S., 2014. Wave attenuation over coastal salt
 682 marshes under storm surge conditions. *Nature Geoscience* 7, 727-731.
- 683 Moller, I., Spencer, T., 2002. Wave dissipation over macro-tidal saltmarshes: Effects of marsh edge
 684 typology and vegetation change. *Journal of Coastal Research*, 506-521.
- 685 Moreno-Mateos, D., Power, M.E., Comin, F.A., Yockteng, R., 2012. Structural and Functional Loss in
 686 Restored Wetland Ecosystems. *Plos Biology* 10.

- 687 Morzaria-Luna, L., Callaway, J.C., Sullivan, G., Zedler, J.B., 2004. Relationship between topographic
688 heterogeneity and vegetation patterns in a Californian salt marsh. *15*, 523-530.
- 689 Mossman, H.L., Davy, A.J., Grant, A., 2012. Does managed coastal realignment create saltmarshes
690 with 'equivalent biological characteristics' to natural reference sites? *Journal of Applied Ecology* *49*,
691 1446-1456.
- 692 Reid, M.K., Spencer, K.L., 2009. Use of principal components analysis (PCA) on estuarine sediment
693 datasets: The effect of data pre-treatment. *Environmental Pollution* *157*, 2275-2281.
- 694 Rotman, R., Naylor, L., McDonnell, R., MacNiocaill, C., 2008. Sediment transport on the Freiston
695 Shore managed realignment site: An investigation using environmental magnetism. *Geomorphology*
696 *100*, 241-255.
- 697 Rupperecht, F., Moller, I., Paul, M., Kudella, M., Spencer, T., van Wesenbeeck, B.K., Wolters, G.,
698 Jensen, K., Bouma, T.J., Miranda-Lange, M., Schimmels, S., 2017. Vegetation-wave interactions in salt
699 marshes under storm surge conditions. *Ecological Engineering* *100*, 301-315.
- 700 Spencer, K.L., Carr, S.J., Diggins, L.M., Tempest, J.A., Morris, M.A., Harvey, G.L., 2017. The impact of
701 pre-restoration land-use and disturbance on sediment structure, hydrology and the sediment
702 geochemical environment in restored saltmarshes. *Science of The Total Environment* *587-588*, 47-
703 58.
- 704 Spencer, K.L., Cundy, A.B., Croudace, I.W., 2003. Heavy metal distribution and early-diagenesis in salt
705 marsh sediments from the Medway Estuary, Kent, UK. *Estuarine Coastal and Shelf Science* *57*, 43-54.
- 706 Spencer, K.L., Cundy, A.B., Davies-Hearn, S., Hughes, R., Turner, S., MacLeod, C.L., 2008.
707 Physicochemical changes in sediments at Orplands Farm, Essex, UK following 8 years of managed
708 realignment. *Estuarine Coastal and Shelf Science* *76*, 608-619.
- 709 Strahler, A.N., 1957. Quantitative analysis of watershed geomorphology. *Transactions American*
710 *Geophysical Union* *38*, 913-920.
- 711 Sullivan, M.J.P., Davy, A.J., Grant, A., Mossman, H.L., 2017. Is saltmarsh restoration success
712 constrained by matching natural environments or altered succession? A test using niche models.
713 *Journal of Applied Ecology*, n/a-n/a.
- 714 Symonds, A.M., Collins, M.B., 2005. Sediment dynamics associated with managed realignment;
715 Freiston shore, the wash, UK.
- 716 Tempest, J.A., Harvey, G.L., Spencer, K.L., 2015. Modified sediments and subsurface hydrology in
717 natural and recreated salt marshes and implications for delivery of ecosystem services. *Hydrological*
718 *Processes* *29*, 2346-2357.
- 719 van Proosdij, D., Lundholm, J., Neatt, N., Bowron, T., Graham, J., 2010. Ecological re-engineering of a
720 freshwater impoundment for salt marsh restoration in a hypertidal system. *Ecological Engineering*
721 *36*, 1314-1332.
- 722 Virgin, S.D.S., Beck, A.D., Boone, L.K., Dykstra, A.K., Ollerhead, J., Barbeau, M.A., McLellan, N.R.,
723 2020. A managed realignment in the upper Bay of Fundy: Community dynamics during salt marsh
724 restoration over 8 years in a megatidal, ice-influenced environment. *Ecological Engineering* *149*,
725 105713.
- 726 Wolanski, E., Elliott, M., 2016. *Estuarine Ecohydrology (Second Edition)*. Elsevier, Boston.
- 727 Wolters, M., Garbutt, A., Bakker, J.P., 2005. Salt-marsh restoration: evaluating the success of de-
728 embankments in north-west Europe. *Biological Conservation* *123*, 249-268.
- 729 Zwolsman, J.J.G., Berger, G.W., Vaneck, G.T.M., 1993. Sediment accumulation rates, historical input,
730 postdepositional mobility and retention of major elements and trace-metals in salt-marsh sediments
731 of the Scheldt estuary, SW Netherlands. *Marine Chemistry* *44*, 73-94.

732

733

- Sedimentological processes in a none engineered managed realignment sites investigated
- Results indicated a sedimentation rate of between 30 to 75 mm / year.
- Similar geochemical profiles to natural sites identified.
- Findings inform the design of future sites for maximum ecosystem service delivery.

Journal Pre-proof

Declaration of interests

The authors declare that they have no known competing financial interests or personal relationships that could have appeared to influence the work reported in this paper.

The authors declare the following financial interests/personal relationships which may be considered as potential competing interests:

Journal Pre-proof